This is the author accepted manuscript of: Liu, Q., Liu, C., Meng, Q., Su, B., Ye, H., Chen, B., Li, W., Cao, X., Nie, W., & Ma, N. (2024). Machine learning reveals biological activities as the dominant factor in controlling deoxygenation in the South Yellow Sea. *Continental Shelf Research*, *283*, Article 105348. Advance online publication. https://doi.org/10.1016/j.csr.2024.105348

Machine learning reveals biological activities as the dominant factor in controlling deoxygenation in the South Yellow Sea

Qingyi Liu[1], Chunli Liu[1, 2*], Qicheng Meng[2, 3], Bei Su[4], Haijun Ye[5], Bingzhang Chen[6], Wei Li[1], Xinyu, Cao[1], Wenlong Nie[1], Nina Ma[1]

[1]Marine College, Shandong University (Weihai), Weihai, 264209, China

[2]State Key Laboratory of Satellite Ocean Environment Dynamics, Second Institute of Oceanography, Ministry of Natural Resources, Hangzhou, China

[3]Observation and Research Station of Yangtze River Delta Marine Ecosystems, Ministry of Natural Resources, Zhoushan, China

[4]Institute of Marine Science and Technology, Shandong University, Qingdao, Shandong, 266237, China

[5]State Key Laboratory of Tropical Oceanography, Guangdong Key Laboratory of Ocean Remote Sensing, South China Sea Institute of Oceanology, Chinese Academy of Sciences, Guangzhou 510301, China;

[6]Department of Mathematics and Statistics, University of Strathclyde, Glasgow, G11XQ, UK

*Corresponding author: Chunli Liu (chunliliu@sdu.edu.cn)

Running Head：Biological activities control deoxygenation.

Keywords: Machine learning; Dissolved oxygen; Biological activities; Phytoplankton bloom; Random Forest

This is the author accepted manuscript of: Liu, Q., Liu, C., Meng, Q., Su, B., Ye, H., Chen, B., Li, W., Cao, X., Nie, W., & Ma, N. (2024). Machine learning reveals biological activities as the dominant factor in controlling deoxygenation in the South Yellow Sea. *Continental Shelf Research*, *283*, Article 105348. Advance online publication. https://doi.org/10.1016/j.csr.2024.105348

Abstract:

Dissolved oxygen (DO) is a crucial element for both biotic and abiotic processes in marine ecosystems, but has declined globally in recent decades. Therefore, there is an urgent need for solid large-scale and continuous estimation of DO concentration in vital ecosystems, such as coastal areas. A random forest (RF) model for DO in South Yellow Sea (SYS) was developed by integrating satellite data and simulation data during 2011–2019. The root mean squared error (RMSE) for the training and test sets were 0.514 mg/L and 0.732 mg/L, respectively. Spatiotemporal distributions of DO of multiple layers in the study area during 2011–2019 were very well reproduced by the RF model and showed a slight decline trend in most SYS areas, while more intense decline occurred in the deep central SYS. The analysis of the mechanisms of DO decline in the South Yellow Sea cold water mass (SYSCWM), located in the deep central SYS, indicates that the deoxygenation here is largely due to biological activities. This finding may have implications for studies on drivers of deoxygenation in coastal areas. Furthermore, integrating satellite data with machine learning models can offer a powerful approach to capturing the continuous spatiotemporal characteristics of ocean parameters over large spatial scales.

1. Introduction

Dissolved oxygen (DO) concentration in seawater is a crucial parameter that impacts both biotic and abiotic processes. It influences the growth, reproduction, and feeding of organisms (Batziakas et al., 2020; Flint et al., 2015; Fock and Czudaj, 2019), while also playing a crucial role in regulating biogeochemical cycles involving carbon, nitrogen, and many other elements (Banks et al., 2012; Codispoti et al., 2001; Levin, 2018; Lonborg et al., 2020; Mathew et al., 2022). However, global warming has led to the heating of seawater and stronger stratification; in the meantime, rising nutrient loads resulted in increased productivity in the upper water column. All of this caused increased oxygen consumption, leading to “deoxygenation” in the ocean (Breitburg et al., 2018; Fennel and Testa, 2019; Keeling and Garcia, 2002). The DO content in the global ocean has declined by over 2% since 1960 (Schmidtko et al., 2017), with coastal waters experiencing worse deoxygenation than the open ocean in recent decades (Gilbert et al., 2010). This decline in DO at the coastal water poses a potential threat to marine ecosystem health, which could ultimately impact not only the well-being of marine life but also the livelihoods of approximately 10-12% of the global population who rely directly on marine resources for their survival and economic activities (Wenning, 2020). Despite growing attention to the issue, there is a strong lack of continuous dataset to help fully understand its underlying mechanisms and quantify its declining rates, especially in the marginal seas.

Traditionally, DO concentrations have been measured using titration facilitated by cruises (Bushinsky et al., 2016; Edwards et al., 2010). However, this approach is labor-intensive and costly, and is also subject to weather conditions. Even with improved accessibility, Argo floats face challenges in achieving large-scale, continuous observations. In this context, numerical simulations can be valuable, especially when a significant amount of *in-situ* data have been collected. At present, numerical simulation methods used for DO estimation include process-based (mechanistic) models and data-driven models. Process-based models, such as high-resolution numerical simulation models, can effectively reproduce real-world scenarios through extensive calculations across the entire spatial extent of the study area (Scully, 2013; Xu et al., 2011). Even though such models may provide higher accuracy, they demand extensive multidisciplinary knowledge of the specific study area and are not easily adjustable. By contrast, data-driven models have emerged as a promising approach. They demonstrate significant potential for high efficiency in various fields (Beyan and Browman, 2020; Chen et al., 2020; Goldstein et al., 2019; Malde et al., 2020; Pahlevan et al., 2022; Rubbens et al., 2023; Xiao et al., 2019). When combined with satellite data at high spatiotemporal resolution, these models have been proven effective in modeling DO concentrations (Sadaiappan et al., 2023). For example, Guo et al. (2021) used support vector regression (SVR) to predict DO concentration at the surface of lakes. Li et al. (2023b) employed multiple machine learning models to reproduce hypoxia events in the bottom of the Gulf of Mexico. All of this shows that machine learning performs well at DO simulation. If machine learning methods can be integrated with some marginal seas where DO is at risk of declining, it may offer enlightening information.

The South Yellow Sea (SYS) is a significant marginal sea in the western Pacific Ocean, providing crucial ecological and economic services (Barbier et al., 2011; Dong, 2019; Hou et al., 2020; Long et al., 2023; Yu et al., 2022). However, it is experiencing local deoxygenation (Lin et al., 2005; Wei et al., 2021), and this has a significant impact on the marine ecosystem. The South Yellow Sea Cold Water Mass (SYSCWM) in the SYS plays a vital role in its hydrodynamics and significantly affects its primary production (Guo et al., 2020a; Li et al., 2019), maintaining high DO concentration (> 6 mg/L) year around (Xin et al., 2013; Zhang et al., 2008). Although recent reports suggest warming in the SYSCWM (Yang et al., 2023), the trend in DO concentration remains uncertain. Moreover, it is unknown whether deoxygenation is taking place in the entire SYS and what its driving mechanisms. Existing studies on deoxygenation mechanisms often focus on solubility changes, with less emphasis on the role of biological processes (Oschlies et al., 2018). Thus, we aim to gather large-scale DO data alongside biomass data from satellite observations to explore the mechanisms involved. Using machine learning to generate such DO data is a suitable choice.

Therefore, we developed a machine learning model for reproducing DO concentration in the SYS during 2011–2019. We evaluated four models and 15 sets of inputs, identified the optimal model, and applied it to generate a high-resolution (1/12°) multi-layer map of DO concentration in the SYS. Through analyzing the model outputs, this study aims to determine the spatial and temporal distributions of DO in the SYS, assess whether DO levels are declining, especially in the SYSCWM region, and understand the roles of warming and biological activities in the DO change. This study may have implications for studies on drivers of deoxygenation in the SYS and other coastal areas.

2. Data and Methodology

2.1 Study area

The study area includes the SYS and parts of the north East China Sea, specifically ranging from the northern boundary of the SYS (marked by a black dashed line in Fig. 1a) to 30°N. The SYS is a semi-enclosed marginal sea bordered by the North Yellow Sea to the north and the East China Sea to the south, constituting a part of the Northwest Pacific Ocean. It has an average depth of 44 m (Liu et al., 2009). The coastal areas of Jiangsu and Shandong provinces are of great significance for coastal aquaculture, while most of the SYS shows potential for deep-sea aquaculture (Hou et al., 2020; Yu et al., 2022). The prevailing ocean currents in this region follows a counterclockwise pattern. There is the strong northwestward YSWC in the central area and southward YSCC along the western coasts (Naimie et al., 2001). This circulation pattern results in relatively high temperature in the central SYS during winter. In the deep central SYS, the SYSCWM undergoes seasonal formation, weakening, and disappearance from summer to winter.

This is the author accepted manuscript of: Liu, Q., Liu, C., Meng, Q., Su, B., Ye, H., Chen, B., Li, W., Cao, X., Nie, W., & Ma, N. (2024). Machine learning reveals biological activities as the dominant factor in controlling deoxygenation in the South Yellow Sea. *Continental Shelf Research*, *283*, Article 105348. Advance online publication. https://doi.org/10.1016/j.csr.2024.105348

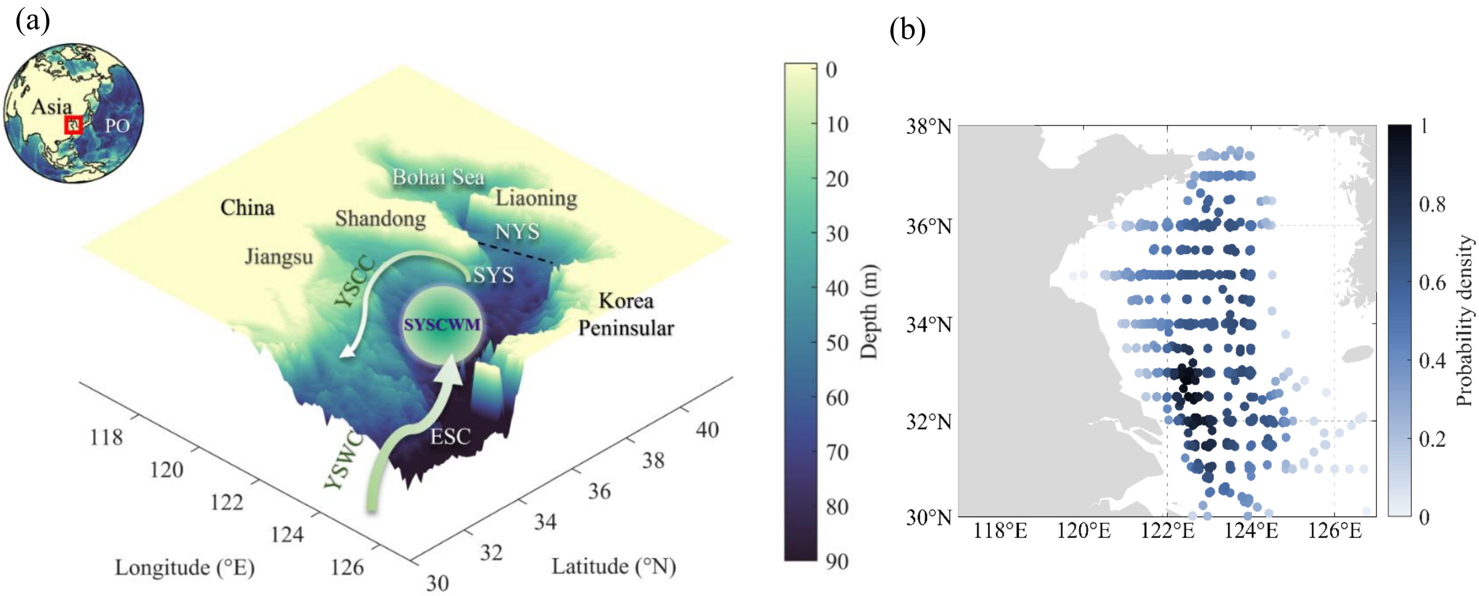

Fig. 1 (a) Geographic location and topography of the study area (NYS: North Yellow Sea; ECS: East China Sea; YSWC: Yellow Sea Warm Current; YSCC: Yellow Sea Coastal Current) and (b) Distribution of *in-situ* DO samples by horizontal location.

2.2 Data

2.2.1 In-situ data

The *in-situ* DO concentration data (3214 data points) used for modeling were compiled from previous studies, including some from the National Earth System Science Data Center (http://www.geodata.cn/index.html). Details about the data source can be found in Table S1. Data samples show a higher frequency in Jun and Aug (usually when DO is low) as shown in Fig. S1a. Spatially, the distribution of samples adequately covers the entire study area (Fig. 1b) and both above and below the mixed layer depth (MLD) (Fig. S1b). The climatological seawater temperature at the vertical profile relating to the DO in Section 4 was obtained from the Regional Climatological Dataset of East Asia (RCDEA; https://www.ncei.noaa.gov/products/regional-ocean-

This is the author accepted manuscript of: Liu, Q., Liu, C., Meng, Q., Su, B., Ye, H., Chen, B., Li, W., Cao, X., Nie, W., & Ma, N. (2024). Machine learning reveals biological activities as the dominant factor in controlling deoxygenation in the South Yellow Sea. *Continental Shelf Research*, *283*, Article 105348. Advance online publication. https://doi.org/10.1016/j.csr.2024.105348

climatologies).

2.2.2 Satellite data

The 8-day sea surface temperature (SST) satellite data at a resolution of 4 km during 2011–2019 were extracted from level-3 product of MODIS Aqua Ocean Color Data, produced by NASA's Earth Observing System Data and Information System (EOSDIS; https://oceancolor.gsfc.nasa.gov/). The 8-day sea surface Chlorophyll-a (Chl-*a*) concentration data at 4 km resolution were obtained from Ocean Color-CCI (OC-CCI), which provides Chl-*a* multi-satellite fusion products from a blended combination of OCI, OCI2, OC2 and OCx algorithms (https://www. oceancolour. org/).

To enhance the model's accuracy and validity, we conducted Data Interpolating Empirical Orthogonal Functions (DINEOF) interpolation(Li et al., 2023a; Niu et al., 2021) to fill in missing pixels (caused by weather or technology) and aligned the DO samples with corresponding satellite observations from the same week (8 days). The coefficient of variation (CV) of the 3*3 window was restricted to within 20% to filter sensor and algorithm noises. Data that not meet this criterion were excluded (about 3.76%). Additional details about the data can be found in Table 1.

Table 1 Data sources used in this study.

Variables	Data Product	Temporal Resolution	Spatial Resolution
In-situ DO	(Present study)	/	/
Modeling DO	GOBH	Daily	1/4°
SST	MODIS-Aqua	8-day	4km

Seawater temperature	RCDEA	Monthly climatological	1/10°
	GLORYS	Monthly	1/12°
Chl-*a*	OC-CCI	8-day	4 km
MLD	GLBu0.08	8-day	1/12°

2.2.3 Simulated data acquisition and processing

8-day composite MLD data at a resolution of 1/12° were derived from GLBu0.08 from the Hybrid Coordinate Ocean Model (HYCOM; https://www.hycom.org/). The simulated DO concentration data were obtained from the Global Ocean Biogeochemistry Hindcast (GOBH) model, produced by the Copernicus Marine Environment Monitoring Service (CMEMS; http://marine.copernicus.eu/) and were used for comparison with our model. Monthly three-dimensional seawater temperature and salinity data were obtained from the Global Ocean Physics Reanalysis (GLORYS) product from the CMEMS and were used to define the SYSCWM region. This region was defined as areas within the 10 °C isotherm at the bottom layer for a given month.

2.3 Models

The model selection and development procedures are illustrated in Fig. 2a, with more detailed steps are shown in Fig. 2b. The model selection included 15*4*50 independent simulations. The number 15 represents the number of input variable sets. Each set consists of SST, water depth, MLD, Chl-*a*, and time (coded by an integer). In every set, only the Chl-*a* varies while the other variables stay unchanged. We focused on the cumulative effect of surface Chl-*a* prior to *in-situ* DO. Subsequently, Chl-*a* from

This is the author accepted manuscript of: Liu, Q., Liu, C., Meng, Q., Su, B., Ye, H., Chen, B., Li, W., Cao, X., Nie, W., & Ma, N. (2024). Machine learning reveals biological activities as the dominant factor in controlling deoxygenation in the South Yellow Sea. *Continental Shelf Research*, *283*, Article 105348. Advance online publication. https://doi.org/10.1016/j.csr.2024.105348

0 to 14 weeks before *in-situ* DO was extracted. Then, 15 means of Chl-*a* averaged over specific weeks were imputed for selection, as Chl-*a* has a delayed effect on DO with different time lags (Zheng and DiGiacomo, 2020). The number 4 represents four modeling methods, i.e., RF, SVR, Generalized Regression Neural Network (GRNN) and Stepwise Linear Regression (SR). These models have been demonstrated to be effective in predicting DO in multiple previous studies (Guo et al., 2021; Heddam, 2014; Ji et al., 2017; Li et al., 2023b; Valera et al., 2020). Detailed information about the structure and principles of the four models can be found in the supplementary materials.

For each of the 15*4 choices, a model was developed and repeated 50 times. In each iteration, input and output variables were randomly divided into a training set (70% of data points) and a test set (30% of data points) using a hierarchical random sampling method. The data in the training set were used for modeling, while the data in the test set were employed for evaluation. The average root mean square error (RMSE, Eq. (S1)) and average correlation coefficient (R, Eq. (1)) of the test set from 50 simulations were calculated and recorded.

$$\mathrm{R} = \frac{\sum_{i=1}^{N}(y_i-\bar{y}_i)*(\hat{y}_i-\bar{\hat{y}}_i)}{\sqrt{\sum_{i=1}^{N}(y_i-\bar{y}_i)^2*(\hat{y}_i-\bar{\hat{y}}_i)^2}} \tag{1}$$

Where N represents the number of the match-up pairs, y_i, $\bar{y}_i$, $\hat{y}_i$, and $\bar{\hat{y}}_i$ are the *in-situ*, mean *in-situ*, simulated, and mean simulated DO concentrations, respectively.

This is the author accepted manuscript of: Liu, Q., Liu, C., Meng, Q., Su, B., Ye, H., Chen, B., Li, W., Cao, X., Nie, W., & Ma, N. (2024). Machine learning reveals biological activities as the dominant factor in controlling deoxygenation in the South Yellow Sea. *Continental Shelf Research*, *283*, Article 105348. Advance online publication. https://doi.org/10.1016/j.csr.2024.105348

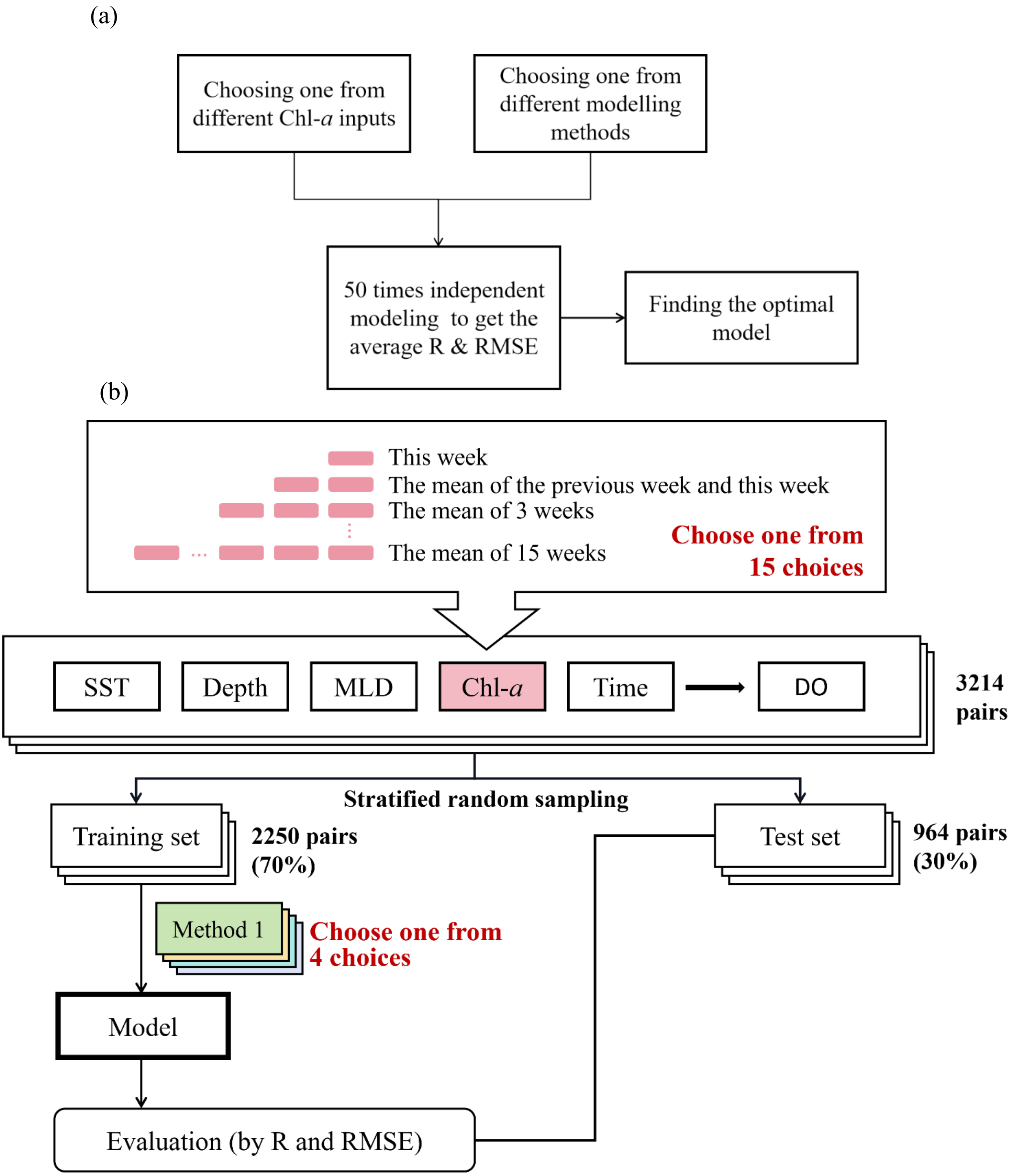

187 **Fig. 2** Sketch diagrams showing (a) overall procedures of model selection and (b) the detailed

188 procedures of modeling.

3. Results

3.1 Performance of models

The RF model, which used the mean of 8 weeks' Chl-*a* as one of the input variables, produces the lowest RMSE and highest R values. This indicates its superior performance compared to the other models (Fig. S2). The results predicted by the RF model closely match the *in-situ* DO observations (Fig.S2b), confirming its effectiveness. Hence, we selected the RF model with the 8 weeks mean Chl-*a* concentration as one input variable as our final model. However, when comparing its performance on the test set with training dataset, we observe slight overfitting of the RF model to the training data (Fig. 3). In Fig. 3b, some outliers appear in the low DO segment (< 4mg/L), indicating that the model overestimates DO in this range. Despite of this defect, the model demonstrates reliable performance in both the training and test sets, with RMSE < 0. 8 mg/L, R > 0. 95, and mean absolute error (Eq. S2) < 0. 5 mg/L. We also compared the model performances above and below the MLD. Both regions exhibit a similar ability to the overall model (Fig. S3), indicating consistent performance across different

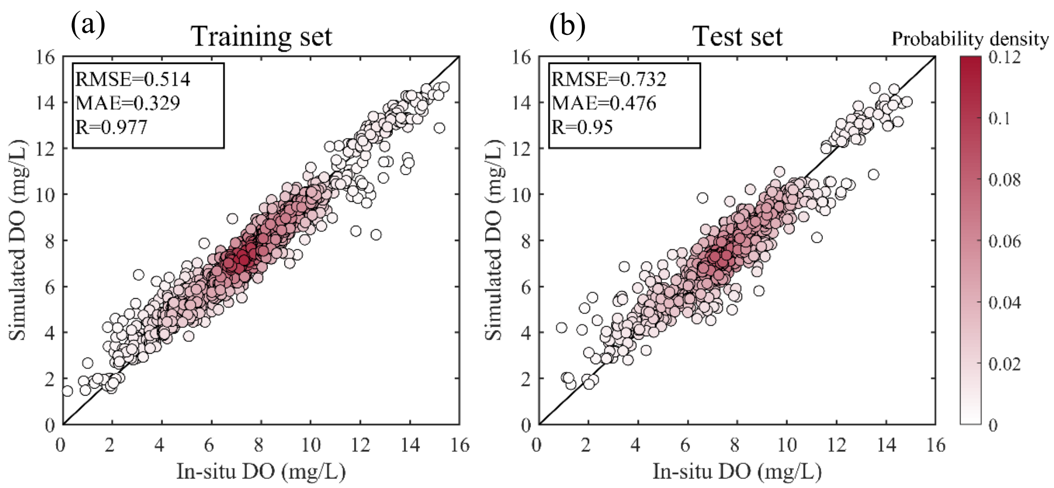

water depths.

Fig. 3 Scatter plots of results of the RF model alongside the *in-situ* data. (a) Training set, (b) Test set.

3.2 Variation of Monthly DO during 2011–2019

The monthly climatological DO derived from the model outputs during 2011–2019 reveals that DO generally decreased from the inshore to the center of the SYS and from the upper layer to the deeper layer in most months (Fig. 4). However, above the 10 m layer from Jun to Sep, DO increases from the inshore to the center of the SYS. In addition, both the surface and the 10 m layers show prominent bands of high DO inshore in most months, especially from Apr to Jun. Furthermore, from Jun to Aug, an area with DO higher than both the upper and deeper layers is displayed at the 30 m layer in the center of the SYS.

The DO in the SYS also exhibits significant seasonal variations. Generally, DO exhibits a gradual decline from late winter (Jan, Feb) to midsummer (Aug), followed by a subsequent increase after early autumn (Sep, Oct). The lowest DO levels are observed in August, while the highest levels occur in Mar. However, the recovery of DO does not take place during autumn (Sep, Oct, and Nov) in the center of the SYS (SYSCWM region) at a depth of 60 m.

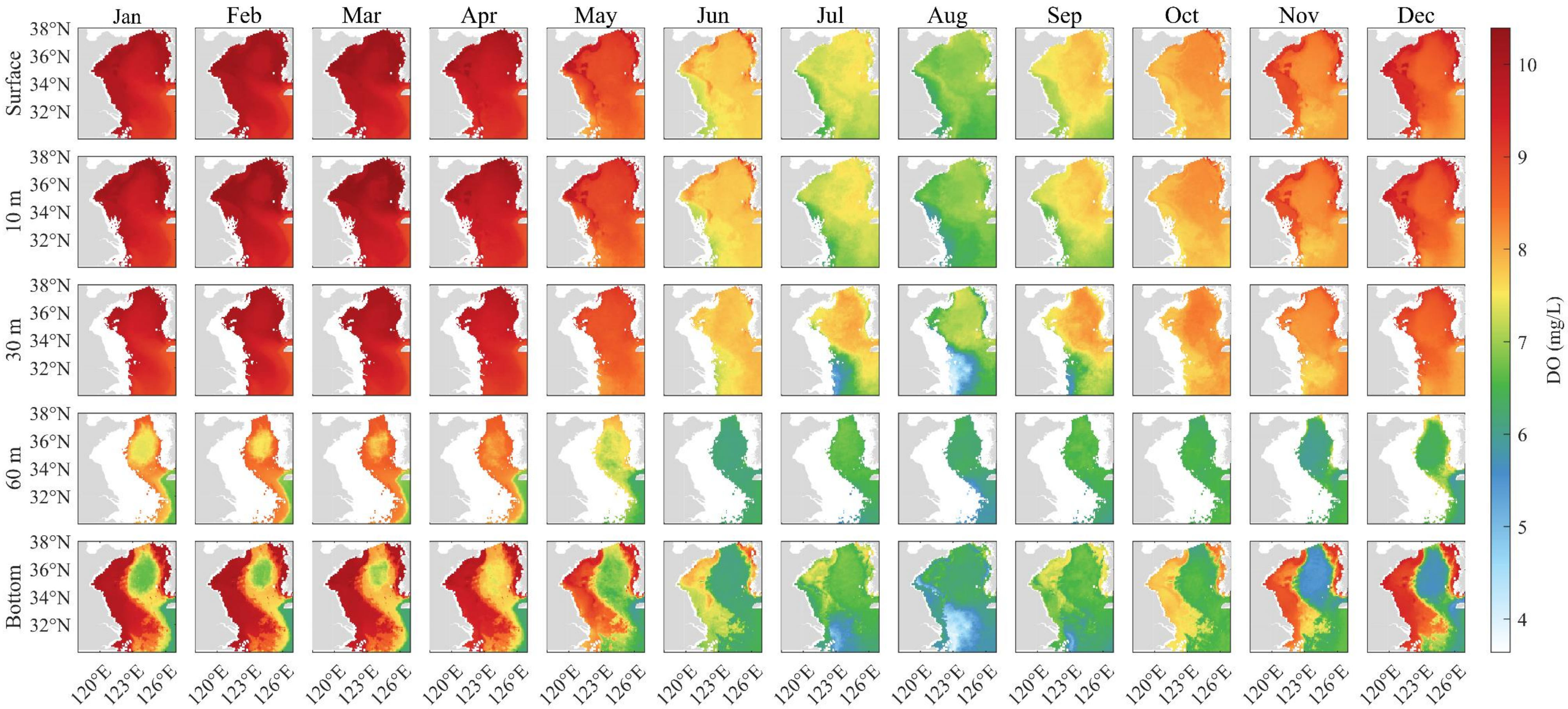

Fig. 4 Simulated monthly climatological DO concentrations from Jan 2011‒Dec 2019. The surface and bottom layers are defined as the layer with a depth of 1 m and the depth of the seabed topography, respectively.

3.3 Long-term patterns of DO during 2011–2019

The long-term temporal variations of DO across different layers were analyzed during 2011–2019. By using the slope coefficient of a linear regression model as an indicator of the change extent, the spatial trends in DO were determined. During 2011–2019, DO in the SYS show a slight downward trend, ranging from 0.0712 to 0.277 mg/L per year. A more profound decrease is observed at deeper layers compared to the surface (Fig. 5a). Particularly noteworthy is the significant downward trend below the 60 m layer of the center of the SYS, where the seasonal SYSCWM typically forms. We further divided the water column above and below the MLD in the SYSCWM region using the simulated MLD data (the well-known SYSCWM is typically found below the MLD in this division). Then, the DO trends above and below the MLD in the SYSCWM region were analyzed, revealing a consistent decline in both regions, with a more pronounced decline in DO below the MLD (Fig. 5b). This suggests the possibility of different regulating mechanisms.

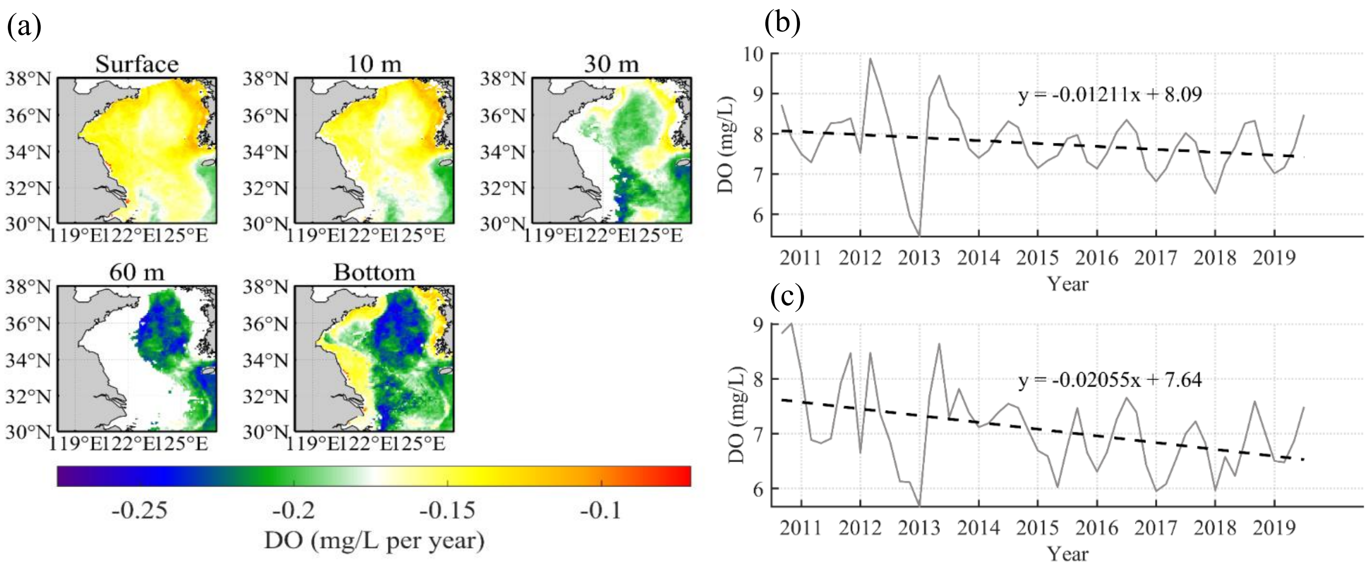

This is the author accepted manuscript of: Liu, Q., Liu, C., Meng, Q., Su, B., Ye, H., Chen, B., Li, W., Cao, X., Nie, W., & Ma, N. (2024). Machine learning reveals biological activities as the dominant factor in controlling deoxygenation in the South Yellow Sea. *Continental Shelf Research*, *283*, Article 105348. Advance online publication. https://doi.org/10.1016/j.csr.2024.105348

Fig. 5 Long-term trend of DO. (a) Spatial patterns and (b, c) temporal evolutions of DO concentrations in the SYSCWM region (b) Above the MLD, (c) Below the MLD (the DO concentration from the model, with a vertical resolution of 1 m, was monthly averaged above and below the MLD). The period shown in (b, c) only includes the DO of Jun to Nov each year. During this period, a closure of the SYSCWM region can be identified in most of the years. In (b) and (c), missing values were replaced by interpolated values.

4. Discussion

4.1 Mechanisms underlying the spatiotemporal patterns of DO

We observe close relationship between SST and DO, as evident from Figs. 4 and S4. DO shows a gradual decline from late winter (Jan, Feb) to midsummer, followed by an increase after early autumn (Sep, Oct). Meanwhile, SST increases from early spring (Mar) and declines after autumn (Sep). This negative correlation is mainly explained by the lower DO solubility in warmer seawater. In addition, enhanced stratification caused by high seawater temperature at the surface can also limit ventilation into deep water, leading to depletion of DO at the bottom. In Jan and Feb, the dominant current patterns of YSCC and YSWC result in high seawater temperature in the central region and low temperatures inshore. The spatial patterns of DO at surface, 10 m and 30 m layers in these months closely match the patterns of SST (Fig. S4), with high DO inshore and low DO in the center of the SYS. This indicates that DO in these months is primarily driven by seawater temperature. This is likely due to the well-mixed water column in winter (Fig. S5), leading to sufficient replenishment of DO, thus following the oxygen solubility (Wei et al., 2021). From Jun to Sep, there is a reversal in the trend in the upper layers, with lower DO inshore. This can be attributed to the shallow water depth in the Subei Shoal, resulting in elevated seawater temperatures. The strong correlation of SST and DO is further supported by the fact that SST emerges as a significant factor among all variables considered in our model (Fig. S6).

DO concentrations are significantly influenced by biological activities such as photosynthesis and respiration. The presence of a high DO band inshore at the surface and 10 m layers is evident from Apr to Jun. This can be attributed to phytoplankton blooms, which is supported by the frequent observation of green tides in Subei Shoal from May to Jul (Hu et al., 2010; Wei et al., 2018). In early spring, phytoplankton growth is stimulated by favorable seawater temperature and light. At the same time, nutrient supplies are enhanced by stronger vertical mixing. This leads to subsequent DO production through photosynthesis (Niu et al., 2021). During summer, the maximum DO is found in the middle depth of the SYS, particularly from Jul to Sep as shown in Fig. 4. The maximum DO concentration is typically found at around 30 m in the center of the SYS during summer (Wei et al., 2010). At this depth, cold water exists due to strong stratification (Fig. S7), which prevents mixing with the adjacent upper and lower layers. In addition, higher Chl-*a* levels are also found at this depth, suggesting that phytoplankton may contribute to the high DO levels in this region (Zheng et al., 2006). However, this phenomenon gradually diminished as the MLD became deeper (Fig. S5). A sustained low DO concentration in the deep central SYS is observed under the 60 m layer in the following months. This can be attributed to the persistence of the stratification until Nov (Fig. S7). In the absence of sufficient ventilation, DO in deep water is depleted by the remineralization of sinking organic particles.

4.2 Mechanisms of DO decline in the SYSCWM

Even though our results suggest that seasonal DO variations are highly correlated with seasonal seawater temperature changes in Section 4.1, the long-term downward trend in the center of the SYS is not solely caused by rising temperature. Thus, we used a computational method to separate the effect of biological activities and warming on deoxygenation. The details of this method are described in the supplementary materials.

In the SYSCWM region, either above or below the MLD, the primary factor accounting for decline in DO is the biological activity (Table S2). These could be interpreted as either a decline in oxygen production or an increase in oxygen consumption. Above the MLD in the water column, DO often appears oversaturated as phytoplankton thrives under optimal temperature and light conditions (Wei et al., 2021). This suggests that the decline in DO above the MLD can be attributed to a decrease in oxygen production during photosynthesis. Below the MLD in the water column, the decline in DO may be attributed to the more intense oxygen consumption of sinking organic particles through respiration. To see if phytoplankton biomass is changing as expected, the trends of sea surface Chl-*a* at the annual and monthly scales were plotted respectively (Fig. 6, S8).

After examining the trend of the sea surface Chl-*a*, a declining trend was found during 2011–2019 in the central SYS both in annual scale and most month (Fig. S8), which aligns with our inferences above the MLD. But this trend seems to contradict the decline in DO below the MLD. However, from the monthly Chl-*a* trend, we find that it has an upward trend in spring. Fig. 6 shows a clear increasing trend in Chl-*a* in the center of the SYS (the SYSCWM region) in Feb and Mar, especially in Mar. This indicates that particles formed from a luxuriant phytoplankton bloom in early spring may sink and consume DO below the MLD, thereby reducing DO in the deep water in next several months. Some studies show a similar phenomenon that organic particles produced from the phytoplankton blooms in spring may exacerbate depletion of DO at the bottom, and the oxygen consuming effect may continue from spring into summer (Zheng and DiGiacomo, 2020). Notably, there is also a significant increase in Chl-*a* in some months near the Subei shoal (e.g. June). Although the increase in Chl-*a* in this part may have an effect on the DO below it and, therefore, on the DO in SYSCWM, this effect may be limited by the presence of a seawater temperature front that surrounds the SYSCWM region (Chen, 2009; Hickox et al., 2000).

Fig. 6 Long-term monthly variations of Chl-*a* concentration during 2011–2019.

To investigate whether the biological contribution to the decline in DO in the SYSCWM (i.e., below the MLD in the SYSCWM region) can be attributed to the stronger early spring bloom, we plotted the Chl-*a* in Mar and the DO in Aug in the SYSCWM region (blow the MLD). These months were chosen because they denoted the increase in phytoplankton bloom in early spring and the peak phase of the SYSCWM, respectively. The correlation between them is -0.772 ($P < 0.05$), indicating a plausible link between stronger early spring phytoplankton blooms and reduced DO in the SYSCWM (Fig. S9). We also calculated the correlation between DO in Jun in the SYSCWM and that in Aug ($P < 0.05$). The strong correlation suggests that the low DO

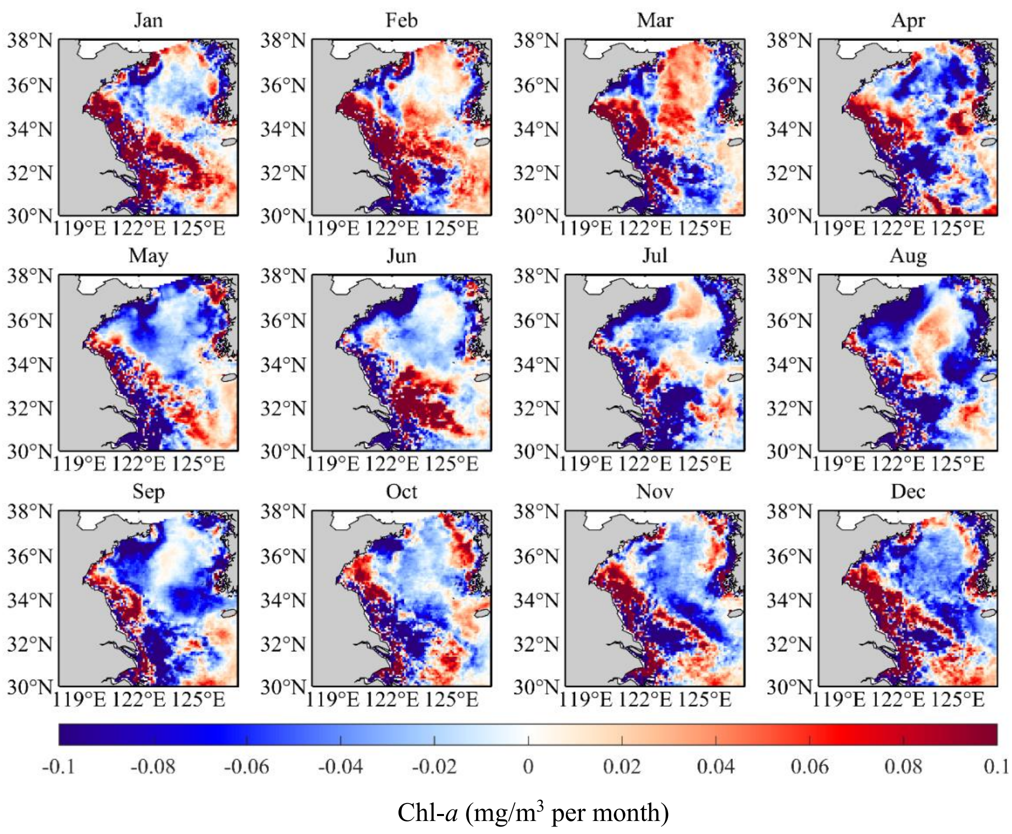

This is the author accepted manuscript of: Liu, Q., Liu, C., Meng, Q., Su, B., Ye, H., Chen, B., Li, W., Cao, X., Nie, W., & Ma, N. (2024). Machine learning reveals biological activities as the dominant factor in controlling deoxygenation in the South Yellow Sea. *Continental Shelf Research*, *283*, Article 105348. Advance online publication. https://doi.org/10.1016/j.csr.2024.105348

in Aug may be due to that in Jun. Similarly, we investigated whether the Chl-*a* in the southern part of the study area in Jun was related to the DO of the SYSCWM. The results showed that there was no significant correlation between them ($p > 0.05$), suggesting the effect of the seawater temperature fronts as a barriers. Collectively, our hypothesis that the organic particles formed in spring may account for the decline in DO in the SYSCWM remains valid. The proposed mechanism is visually represented in Fig. 7.

In addition, physical processes also play a role in this process. For instance, the process illustrated in Fig. 7 may be augmented by the mixed layer pump (MLP) observed in many studies. That is, in regions with significant seasonal variation in the MLD, surface organic particles are pushed into deeper waters by intensified wind mixing during the colder seasons (Lacour et al., 2019; Xing et al., 2020). Stronger stratification due to warming can reduce nutrient supply to the surface, subsequently decreasing primary production (Dave and Lozier, 2013). It can also limit the extent of ventilation from the surface to the deep water. In essence, warming and biological activities can sometimes interact. Aside from directly affecting the DO content entering the ocean (through air-sea exchange), warming can also change DO content by influencing ocean hydrology which then regulates the biological activities.

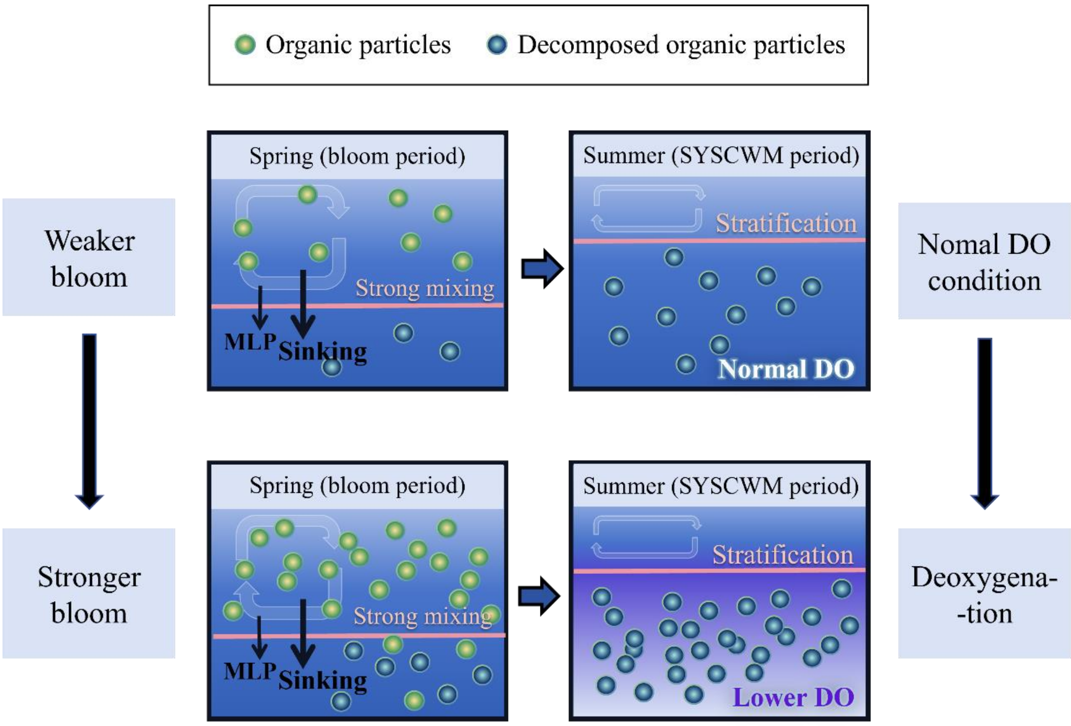

Fig.7 Schematic of the mechanisms of deoxygenation explained by biological activities in the SYSCWM. In spring, stronger phytoplankton blooms formed more sinking particles, while the mixing gradually weakened and the water column gradually stratified in the following months. Then these particles continued to sink and gradually consumed more DO below the MLD through respiration. In summer, or the SYSCWM period, lower DO is present and it is difficult to be replenished from the upper layers of the stratified water column.

In addition to the overall downward trend, there are some details worth our attention in Fig.5, such as DO in the year 2013 is considerably lower than any other years. After plotting the interannual variation of SST in Aug and Chl-*a* in Feb and Mar, we found that 2013 had a higher SST than most years and the highest spring Chl-*a* (Fig. S10) High seawater temperatures and strong stratification, combined with enough sinking particles produced by phytoplankton, contributed to the low DO in summer

This is the author accepted manuscript of: Liu, Q., Liu, C., Meng, Q., Su, B., Ye, H., Chen, B., Li, W., Cao, X., Nie, W., & Ma, N. (2024). Machine learning reveals biological activities as the dominant factor in controlling deoxygenation in the South Yellow Sea. *Continental Shelf Research*, *283*, Article 105348. Advance online publication. https://doi.org/10.1016/j.csr.2024.105348

2013.

4.3 Advantages and drawbacks of the study

Based on extensive previous studies, our modelling study provides distribution and trends of DO with higher spatial-temporal resolution, thus highlighting locations of more intense deoxygenation. The spatial patterns of DO exhibited by our model aligns closely with a substantial body of empirical studies (Guo et al., 2020b; Guo et al., 2020c; Li et al., 2015; Lu et al., 2017; Luo et al., 2018; Qu et al., 2015; Xiong et al., 2020; Zhu et al., 2017). Besides, the declining DO observed by our model in the SYS is consistent with previous findings (Wei et al., 2021), which also show a more significant decline in DO in the deeper layers of the SYS. This further substantiates the reliability of modeling as an approach to comprehensively capture spatiotemporal patterns despite limited *in-situ* data availability. Although global model data with similar functions are available, our model exhibited higher accuracy and higher resolution in comparison to the global model in our study area (Fig. S11). Moreover, the error observed in our study is considered acceptable compared to similar studies, which achieved an RMSE of approximately 1 mg/L (Guo et al., 2021; Kim et al., 2020; Li et al., 2023b; Ross and Stock, 2019).

This study not only captures the spatial and temporal characteristics of DO, but also demonstrates the feasibility of machine learning combined with satellite data to predict the DO concentration in the SYS. This approach would reduce the cost of instruments and labor. However, narrowing down the error caused by potential inaccuracies in satellite data as well as the inherent limitations of the model itself remains a challenging task. Our model may not fully capture the actual variations in extremely low DO conditions (e.g., < 4 mg/L). This can be attributed to the involvement of more intricate processes in DO dynamics in these cases, such as sediment consumption and advection transport. There are also other challenges that remain to be further addressed. For example, the precision of input data and the comprehensiveness of *in-situ* data need improvement. In the future, we anticipate that more *in-situ* data will be collected, satellite data will be accurately calibrated, and additional variables will be incorporated to enhance the precision of the model. Moreover, due to the introduction of the time variable into the model and its significant contribution to the result (Fig. S6), the accuracy of dissolved oxygen simulation beyond the time range cannot be guaranteed. It is expected that the model's time variable will be adjusted or deleted in the future to enhance the usability of the model in forecasting. More discussions on the time variable and the partial correlation curves (Fig. S12) can be found in the supplementary material. Additionally, the potential of the proposed approach for achieving similar performance in other waters remains to be tested.

5. Conclusion

In this study, an RF model was presented to efficiently and accurately simulate the DO conditions of multiple layers in the SYS during 2011–2019. This provided a comprehensive spatiotemporal distribution of DO within the SYS. The model has achieved good accuracy and effectively captures a declining trend of DO in the SYS, with a more significant decline at the deep layers compared to the shallower ones. The decline in DO in the SYSCWM region above and below the MLD was regulated by decreased surface Chl-*a* and stronger early spring phytoplankton blooms, respectively. Although this study focuses on DO in the SYS, the proposed framework and methodology can be readily applied to other coastal systems lacking sufficient *in-situ* data. The findings of the model may serve as a valuable reference for high-resolution modeling studies and other related investigations. Additionally, it can aid in the development of appropriate frameworks for deep-sea aquaculture activities and cruise survey planning.

Data availability statement

Data will be made available on request.

Author Contribution Statement:

Q.L. handled data curation, conceptualization, and wrote the original draft. C.L. supervised, acquired funding, and reviewed/edited. Q.M. acquired funding and reviewed/edited. B.S., H.Y., B.C., and W.L. reviewed/edited. X.C. curated data. W.N. performed formal analysis. N.M. visualized the data.

Declaration of competing interest

The authors declare that they have no competing financial interests or personal relationships that could have appeared to influence the work reported in this paper. All authors have read and agree to the published version of the manuscript.

Acknowledgments

This work is supported by the following research grants: National Natural Science Foundation of China (42230404); Shandong Provincial Natural Science Foundation (ZR2020MD098); Open Fund of State Key Laboratory of Satellite Ocean Environment Dynamics, Second Institute of Oceanography, MNR (QNHX2315).

Reference

Banks, J., Ross, D.J., Keough, M.J., 2012. Short-term (24 h) effects of mild and severe hypoxia (20% and 5% dissolved oxygen) on metal partitioning in highly contaminated estuarine sediments. Estuarine Coastal and Shelf Science, 99: 121-131. http://dx.doi.org/10.1016/j.ecss.2011.12.025

Barbier, E.B., Hacker, S.D., Kennedy, C., Koch, E.W., Stier, A.C., Silliman, B.R., 2011. The value of estuarine and coastal ecosystem services. Ecological Monographs, 81(2): 169-193. http://dx.doi.org/10.1890/10-1510.1

Batziakas, S., Frangoulis, C., Tsiola, A., Nikolioudakis, N., Tsagaraki, T.M., Somarakis, S., 2020. Hypoxia changes the shape of the biomass size spectrum of planktonic communities: a case study in the eastern Mediterranean (Elefsina Bay). Journal of Plankton Research, 42(6): 752-766. http://dx.doi.org/10.1093/plankt/fbaa055

Beyan, C., Browman, H.I., 2020. Setting the stage for the machine intelligence era in marine science. Ices Journal of Marine Science, 77(4): 1267-1273. http://dx.doi.org/10.1093/icesjms/fsaa084

Breitburg, D., Levin, L.A., Oschlies, A., Gregoire, M., Chavez, F.P., Conley, D.J., Garcon, V., Gilbert, D., Gutierrez, D., Isensee, K., Jacinto, G.S., Limburg, K.E., Montes, I., Naqvi, S.W.A., Pitcher, G.C., Rabalais, N.N., Roman, M.R., Rose, K.A., Seibel, B.A., Telszewski, M., Yasuhara, M., Zhang, J., 2018. Declining oxygen in the global ocean and coastal waters. Science, 359(6371): 46-+. http://dx.doi.org/10.1126/science.aam7240

Bushinsky, S.M., Emerson, S.R., Riser, S.C., Swift, D.D., 2016. Accurate oxygen measurements on modified Argo floats using in situ air calibrations. Limnology and Oceanography-Methods, 14(8): 491-505. http://dx.doi.org/10.1002/lom3.10107

Chen, B., Liu, H., Xiao, W., Wang, L., Huang, B., 2020. A machine-learning approach to modeling picophytoplankton abundances in the South China Sea. Progress in Oceanography, 189.

http://dx.doi.org/10.1016/j.pocean.2020.102456

Chen, C.-T.A., 2009. Chemical and physical fronts in the Bohai, Yellow and East China seas. Journal of Marine Systems, 78(3): 394-410. http://dx.doi.org/10.1016/j.jmarsys.2008.11.016

Codispoti, L.A., Brandes, J.A., Christensen, J.P., Devol, A.H., Naqvi, S.W.A., Paerl, H.W., Yoshinari, T., 2001. The oceanic fixed nitrogen and nitrous oxide budgets: Moving targets as we enter the anthropocene? Scientia Marina, 65: 85-105. http://dx.doi.org/10.3989/scimar.2001.65s285

Dave, A.C., Lozier, M.S., 2013. Examining the global record of interannual variability in stratification and marine productivity in the low-latitude and mid-latitude ocean. Journal of Geophysical Research: Oceans, 118(6): 3114-3127. http://dx.doi.org/https://doi.org/10.1002/jgrc.20224

Dong, S., 2019. Researching Progresses and Prospects in Large Salmonidae Farming in Cold Water Mass of Yellow Sea. Periodical of Ocean University of China, 49(3): 1-6.

Edwards, B., Murphy, D., Janzen, C., Larson, N., 2010. Calibration, Response, and Hysteresis in Deep-Sea Dissolved Oxygen Measurements. Journal of Atmospheric and Oceanic Technology, 27(5): 920-931. http://dx.doi.org/10.1175/2009jtecho693.1

Fennel, K., Testa, J.M., 2019. Biogeochemical Controls on Coastal Hypoxia. In: Carlson, C.A., Giovannoni, S.J. (Eds.), Annual Review of Marine Science, Vol 11. Annual Review of Marine Science, pp. 105-130. DOI:10.1146/annurev-marine-010318-095138

Flint, N., Crossland, M.R., Pearson, R.G., 2015. Sublethal effects of fluctuating hypoxia on juvenile tropical Australian freshwater fish. Marine and Freshwater Research, 66(4): 293-304. http://dx.doi.org/10.1071/mf14120

Fock, H.O., Czudaj, S., 2019. Size structure changes of mesopelagic fishes and community biomass size spectra along a transect from the equator to the Bay of Biscay collected in 1966-1979 and 2014-2015. Ices Journal of Marine Science, 76(3): 755-770. http://dx.doi.org/10.1093/icesjms/fsy068

Gilbert, D., Rabalais, N.N., Diaz, R.J., Zhang, J., 2010. Evidence for greater oxygen decline rates in the coastal ocean than in the open ocean. Biogeosciences, 7(7): 2283-2296. http://dx.doi.org/10.5194/bg-7-2283-2010

Goldstein, E.B., Coco, G., Plant, N.G., 2019. A review of machine learning applications to coastal sediment transport and morphodynamics. Earth-Science Reviews, 194: 97-108. http://dx.doi.org/10.1016/j.earscirev.2019.04.022

Guo, C., Zhang, G., Sun, J., Leng, X., Xu, W., Wu, C., Li, X., Pujari, L., 2020a. Seasonal responses of nutrient to hydrology and biology in the southern Yellow Sea. Continental Shelf Research, 206. http://dx.doi.org/10.1016/j.csr.2020.104207

Guo, H., Huang, J.J., Zhu, X., Wang, B., Tian, S., Xu, W., Mai, Y., 2021. A generalized machine learning approach for dissolved oxygen estimation at multiple spatiotemporal scales using remote sensing. Environ Pollut, 288: 117734. http://dx.doi.org/10.1016/j.envpol.2021.117734

Guo, J., Yuan, H., Song, J., Li, X., Duan, L., 2020b. Hypoxia, acidification and nutrient accumulation in the Yellow Sea Cold Water of the South Yellow Sea. Sci Total Environ, 745: 141050. http://dx.doi.org/10.1016/j.scitotenv.2020.141050

Guo, X., Xu, B., Burnett, W.C., Wei, Q., Nan, H., Zhao, S., Charette, M.A., Lian, E., Chen, G., Yu, Z., 2020c. Does submarine groundwater discharge contribute to summer hypoxia in the Changjiang (Yangtze) River Estuary? Sci Total Environ, 719: 137450. http://dx.doi.org/10.1016/j.scitotenv.2020.137450

This is the author accepted manuscript of: Liu, Q., Liu, C., Meng, Q., Su, B., Ye, H., Chen, B., Li, W., Cao, X., Nie, W., & Ma, N. (2024). Machine learning reveals biological activities as the dominant factor in controlling deoxygenation in the South Yellow Sea. *Continental Shelf Research*, *283*, Article 105348. Advance online publication. https://doi.org/10.1016/j.csr.2024.105348

Heddam, S., 2014. Generalized regression neural network-based approach for modelling hourly dissolved oxygen concentration in the Upper Klamath River, Oregon, USA. Environ Technol, 35(13-16): 1650-7. http://dx.doi.org/10.1080/09593330.2013.878396

Hickox, R., Belkin, I., Cornillon, P., Shan, Z., 2000. Climatology and seasonal variability of ocean fronts in the East China, Yellow and Bohai seas from satellite SST data. Geophysical Research Letters, 27(18): 2945-2948. http://dx.doi.org/10.1029/1999gl011223

Hou, J., Zhou, W., Wang, L., Fan, W., Yuan, Z., 2020. Spatial analysis of the potential of deep-sea aquaculture in China. Resources Science, 42(7): 1325-1337.

Hu, C., Li, D., Chen, C., Ge, J., Muller-Karger, F.E., Liu, J., Yu, F., He, M.-X., 2010. On the recurrent Ulva prolifera blooms in the Yellow Sea and East China Sea. Journal of Geophysical Research-Oceans, 115. http://dx.doi.org/10.1029/2009jc005561

Ji, X., Shang, X., Dahlgren, R.A., Zhang, M., 2017. Prediction of dissolved oxygen concentration in hypoxic river systems using support vector machine: a case study of Wen-Rui Tang River, China. Environ Sci Pollut Res Int, 24(19): 16062-16076. http://dx.doi.org/10.1007/s11356-017-9243-7

Keeling, R.F., Garcia, H.E., 2002. The change in oceanic O-2 inventory associated with recent global warming. Proceedings of the National Academy of Sciences of the United States of America, 99(12): 7848-7853. http://dx.doi.org/10.1073/pnas.122154899

Kim, Y.H., Son, S., Kim, H.C., Kim, B., Park, Y.G., Nam, J., Ryu, J., 2020. Application of satellite remote sensing in monitoring dissolved oxygen variabilities: A case study for coastal waters in Korea. Environ Int, 134: 105301. http://dx.doi.org/10.1016/j.envint.2019.105301

Lacour, L., Briggs, N., Claustre, H., Ardyna, M., Dall'Olmo, G., 2019. The Intraseasonal Dynamics of the Mixed Layer Pump in the Subpolar North Atlantic Ocean: A Biogeochemical-Argo Float Approach. Global Biogeochemical Cycles, 33(3): 266-281. http://dx.doi.org/10.1029/2018gb005997

Levin, L.A., 2018. Manifestation, Drivers, and Emergence of Open Ocean Deoxygenation. In: Carlson, C.A., Giovannoni, S.J. (Eds.), Annual Review of Marine Science, Vol 10. Annual Review of Marine Science, pp. 229-260. DOI:10.1146/annurev-marine-121916-063359

Li, H.-M., Zhang, C.-S., Han, X.-R., Shi, X.-Y., 2015. Changes in concentrations of oxygen, dissolved nitrogen, phosphate, and silicate in the southern Yellow Sea, 1980–2012: Sources and seaward gradients. Estuarine, Coastal and Shelf Science, 163: 44-55. http://dx.doi.org/10.1016/j.ecss.2014.12.013

Li, W., Liu, C., Zhai, W., Liu, H., Ma, W., 2023a. Remote sensing and machine learning method to support sea surface pCO2 estimation in the Yellow Sea. Frontiers in Marine Science, 10. http://dx.doi.org/10.3389/fmars.2023.1181095

Li, W., Wang, Z., Huang, H., 2019. Relationship between the southern Yellow Sea Cold Water Mass and the distribution and composition of suspended particulate matter in summer and autumn seasons. Journal of Sea Research, 154. http://dx.doi.org/10.1016/j.seares.2019.101812

Li, Y., Robinson, S.V.J., Nguyen, L.H., Liu, J., 2023b. Satellite prediction of coastal hypoxia in the northern Gulf of Mexico. Remote Sensing of Environment, 284. http://dx.doi.org/10.1016/j.rse.2022.113346

Lin, C., Ning, X., Su, J., Lin, Y., Xu, B., 2005. Environmental changes and the responses of the ecosystems of the Yellow Sea during 1976-2000. Journal of Marine Systems, 55(3-4): 223-234. http://dx.doi.org/10.1016/j.jmarsys.2004.08.001

Liu, Z., Wei, H., Lozovatsky, I.D., Fernando, H.J.S., 2009. Late summer stratification, internal waves, and turbulence in the Yellow Sea. Journal of Marine Systems, 77(4): 459-472. http://dx.doi.org/10.1016/j.jmarsys.2008.11.001

Lonborg, C., Carreira, C., Jickells, T., Anton Alvarez-Salgado, X., 2020. Impacts of Global Change on Ocean Dissolved Organic Carbon (DOC) Cycling. Frontiers in Marine Science, 7. http://dx.doi.org/10.3389/fmars.2020.00466

Long, L., Liu, H., Cui, M., Zhang, C., Liu, C., 2023. Offshore aquaculture in China. Reviews in Aquaculture. http://dx.doi.org/10.1111/raq.12837

Lu, W., Xiang, X., Yang, L., Xu, Y., Li, X., Liu, S., 2017. The temporal-spatial distribution and changes of dissolved oxygen in the Changjiang Estuary and its adjacent waters for the last 50 a. Acta Oceanologica Sinica, 36(5): 90-98. http://dx.doi.org/10.1007/s13131-017-1063-6

Luo, X., Wei, H., Fan, R., Liu, Z., Zhao, L., Lu, Y., 2018. On influencing factors of hypoxia in waters adjacent to the Changjiang estuary. Continental Shelf Research, 152: 1-13. http://dx.doi.org/10.1016/j.csr.2017.10.004

Malde, K., Handegard, N.O., Eikvil, L., Salberg, A.-B., 2020. Machine intelligence and the data-driven future of marine science. Ices Journal of Marine Science, 77(4): 1274-1285. http://dx.doi.org/10.1093/icesjms/fsz057

Mathew, D., Gireeshkumar, T.R., Shameem, K., Furtado, C.M., Arya, K.S., Udayakrishnan, P.B., Balachandran, K.K., 2022. Dynamics of trace metals in sediments of a seasonally hypoxic coastal zone in the southeastern Arabian Sea. Oceanologia, 64(4): 735-748. http://dx.doi.org/10.1016/j.oceano.2022.06.007

Naimie, C.E., Blain, C.A., Lynch, D.R., 2001. Seasonal mean circulation in the Yellow Sea - a model-generated climatology. Continental Shelf Research, 21(6-7): 667-695.

Niu, Y., Liu, C., Lu, X., Zhu, L., Sun, Q., Wang, S., 2021. Phytoplankton blooms and its influencing environmental factors in the southern Yellow Sea. Regional Studies in Marine Science, 47. http://dx.doi.org/10.1016/j.rsma.2021.101916

Oschlies, A., Brandt, P., Stramma, L., Schmidtko, S., 2018. Drivers and mechanisms of ocean deoxygenation. Nature Geoscience, 11(7): 467-473. http://dx.doi.org/10.1038/s41561-018-0152-2

Pahlevan, N., Smith, B., Alikas, K., Anstee, J., Barbosa, C., Binding, C., Bresciani, M., Cremella, B., Giardino, C., Gurlin, D., Fernandez, V., Jamet, C., Kangro, K., Lehmann, M.K., Loisel, H., Matsushita, B., Ha, N., Olmanson, L., Potvin, G., Simis, S.G.H., VanderWoude, A., Vantrepotte, V., Ruiz-Verdu, A., 2022. Simultaneous retrieval of selected optical water quality indicators from Landsat-8, Sentinel-2, and Sentinel-3. Remote Sensing of Environment, 270. http://dx.doi.org/10.1016/j.rse.2021.112860

Qu, B., Song, J., Yuan, H., Li, X., Li, N., Duan, L., Chen, X., Lu, X., 2015. Summer carbonate chemistry dynamics in the Southern Yellow Sea and the East China Sea: Regional variations and controls. Continental Shelf Research, 111: 250-261. http://dx.doi.org/10.1016/j.csr.2015.08.017

Ross, A.C., Stock, C.A., 2019. An assessment of the predictability of column minimum dissolved oxygen concentrations in Chesapeake Bay using a machine learning model. Estuarine, Coastal and Shelf Science, 221: 53-65. http://dx.doi.org/10.1016/j.ecss.2019.03.007

Rubbens, P., Brodie, S., Cordier, T., Destro Barcellos, D., Devos, P., Fernandes-Salvador, J.A., Fincham, J.I., Gomes, A., Handegard, N.O., Howell, K., Jamet, C., Kartveit, K.H., Moustahfid, H., Parcerisas, C.,

This is the author accepted manuscript of: Liu, Q., Liu, C., Meng, Q., Su, B., Ye, H., Chen, B., Li, W., Cao, X., Nie, W., & Ma, N. (2024). Machine learning reveals biological activities as the dominant factor in controlling deoxygenation in the South Yellow Sea. *Continental Shelf Research*, *283*, Article 105348. Advance online publication. https://doi.org/10.1016/j.csr.2024.105348

Politikos, D., Sauzede, R., Sokolova, M., Uusitalo, L., Van den Bulcke, L., van Helmond, A.T.M., Watson, J.T., Welch, H., Beltran-Perez, O., Chaffron, S., Greenberg, D.S., Kuehn, B., Kiko, R., Lo, M., Lopes, R.M., Moeller, K.O., Michaels, W., Pala, A., Romagnan, J.-B., Schuchert, P., Seydi, V., Villasante, S., Malde, K., Irisson, J.-O., 2023. Machine learning in marine ecology: an overview of techniques and applications. Ices Journal of Marine Science, 80(7): 1829-1853. http://dx.doi.org/10.1093/icesjms/fsad100

Sadaiappan, B., Balakrishnan, P., Vishal, C.R., Vijayan, N.T., Subramanian, M., Gauns, M.U., 2023. Applications of Machine Learning in Chemical and Biological Oceanography. Acs Omega, 8(18): 15831-15853. http://dx.doi.org/10.1021/acsomega.2c06441

Schmidtko, S., Stramma, L., Visbeck, M., 2017. Decline in global oceanic oxygen content during the past five decades. Nature, 542(7641): 335-339. http://dx.doi.org/10.1038/nature21399

Scully, M.E., 2013. Physical controls on hypoxia in Chesapeake Bay: A numerical modeling study. Journal of Geophysical Research-Oceans, 118(3): 1239-1256. http://dx.doi.org/10.1002/jgrc.20138

Valera, M., Walter, R.K., Bailey, B.A., Castillo, J.E., 2020. Machine Learning Based Predictions of Dissolved Oxygen in a Small Coastal Embayment. Journal of Marine Science and Engineering, 8(12). http://dx.doi.org/10.3390/jmse8121007

Wei, Q., Wang, B., Yao, Q., Fu, M., Sun, J., Xu, B., Yu, Z., 2018. Hydro-biogeochemical processes and their implications for Ulva prolifera blooms and expansion in the world's largest green tide occurrence region (Yellow Sea, China). Science of the Total Environment, 645: 257-266. http://dx.doi.org/10.1016/j.scitotenv.2018.07.067

Wei, Q., Wei, X., Zhan, R., Liu, L., Zang, J., 2010. Distribution of dissolved oxygen and influence factor in west of Southern Yellow Sea in summer. Marine Environmental Science, 29(6): 808-814.

Wei, Q., Xue, L., Yao, Q., Wang, B., Yu, Z., 2021. Oxygen decline in a temperate marginal sea: Contribution of warming and eutrophication. Sci Total Environ, 757: 143227. http://dx.doi.org/10.1016/j.scitotenv.2020.143227

Wenning, R., 2020. THE STATE OF WORLD FISHERIES AND AQUACULTURE (SOFIA) 2020 REPORT. Integrated Environmental Assessment and Management, 16(5): 800-801.

Xiao, C., Chen, N., Hu, C., Wang, K., Gong, J., Chen, Z., 2019. Short and mid-term sea surface temperature prediction using time-series satellite data and LSTM-AdaBoost combination approach. Remote Sensing of Environment, 233. http://dx.doi.org/10.1016/j.rse.2019.111358

Xin, M., Wang, B., Ma, D., 2013. Chemicohydrographic Characteristics Along the Vertical Section in the Yellow Sea. Advances in Marine Science, 31(3): 377-390.

Xing, X., Wells, M.L., Chen, S., Lin, S., Chai, F., 2020. Enhanced Winter Carbon Export Observed by BGC‐Argo in the Northwest Pacific Ocean. Geophysical Research Letters, 47(22). http://dx.doi.org/10.1029/2020gl089847

Xiong, T.-q., Wei, Q.-s., Zhai, W.-d., Li, C.-l., Wang, S.-y., Zhang, Y.-x., Liu, S.-j., Yu, S.-q., 2020. Comparing Subsurface Seasonal Deoxygenation and Acidification in the Yellow Sea and Northern East China Sea Along the North-to-South Latitude Gradient. Frontiers in Marine Science, 7. http://dx.doi.org/10.3389/fmars.2020.00686

Xu, J., Long, W., Wiggert, J.D., Lanerolle, L.W.J., Brown, C.W., Murtugudde, R., Hood, R.R., 2011. Climate Forcing and Salinity Variability in Chesapeake Bay, USA. Estuaries and Coasts, 35(1): 237-261. http://dx.doi.org/10.1007/s12237-011-9423-5

Yang, J., Liu, C., Sun, Q., Zhai, L., Sun, Q., Li, S., Ai, L., Li, X., 2023. Interannual Variability and Long-Term

Trends in Intensity of the Yellow Sea Cold Water Mass during 1993–2019. Journal of Marine Science and Engineering, 11(10). http://dx.doi.org/10.3390/jmse11101888

Yu, S.-E., Dong, S.-L., Zhang, Z.-X., Zhang, Y.-Y., Sara, G., Wang, J., Dong, Y.-W., 2022. Mapping the potential for offshore aquaculture of salmonids in the Yellow Sea. Marine Life Science & Technology, 4(3): 329-342. http://dx.doi.org/10.1007/s42995-022-00141-2

Zhang, S.W., Wang, Q.Y., Lue, Y., Cui, H., Yuan, Y.L., 2008. Observation of the seasonal evolution of the Yellow Sea Cold Water Mass in 1996-1998. Continental Shelf Research, 28(3): 442-457. http://dx.doi.org/10.1016/j.csr.2007.10.002

Zheng, G., DiGiacomo, P.M., 2020. Linkages Between Phytoplankton and Bottom Oxygen in the Chesapeake Bay. Journal of Geophysical Research: Oceans, 125(2). http://dx.doi.org/10.1029/2019jc015650

Zheng, G., Song, J., Dai, J., Wang, Y., 2006. Distributions of chlorophyll A and carbon fixed strength of phytoplankton in autumn of the southern Huanghai Sea waters. Acta Oceanologica Sinica, 25(3): 68-81.

Zhu, Z.Y., Wu, H., Liu, S.M., Wu, Y., Huang, D.J., Zhang, J., Zhang, G.S., 2017. Hypoxia off the Changjiang (Yangtze River) estuary and in the adjacent East China Sea: Quantitative approaches to estimating the tidal impact and nutrient regeneration. Mar Pollut Bull, 125(1-2): 103-114. http://dx.doi.org/10.1016/j.marpolbul.2017.07.029